

Realization of functionally graded components with an optimized hybrid additive laminated tooling method

DARDAEI JOGHAN Hamed^{1,a*}, AGBOOLA Ololade^{1,b} and TEKKAYA A. Erman^{1,c}

¹Institute of Forming Technology and Lightweight Components (IUL), TU Dortmund University, Baroper Str. 303, Dortmund 44227, Germany

^ahamed.dardaei@iul.tu-dortmund.de, ^bololade.agboola@tu-dortmund.de,

^cerman.tekkaya@iul.tu-dortmund.de

Keywords: Laser Metal Deposition, Sheet Lamination, Press Hardening, Warm Forming

Abstract. The tool tempering method is used to manufacture the functionally graded components. In the manufactured combined tool, one side was enhanced with cooling channels to perform the press hardening process, and the other side of the tool included heating cartridges to practice warm forming. Hybrid additive laminated tooling is used to manufacture the combined tool in a short time, while conventional subtracting methods, such as milling, are costly and time-consuming. Initially, the cooling rate and the heat transfer coefficient of the laser metal deposited area by Ferro55 powder are determined. Also, functionally graded components are manufactured in which, on one side, the 22MnB5 sheets are press-hardened, whereas, on the other side, the blanks were warm formed at different elevated temperatures (150°C, 250°C, 350°C). The results show that besides the concept validation, the cooling rate on the press hardening side is higher than 27 K/s, and hardness values up to ca. 480 HV10 were achieved, while, in the wall of the formed part on the heating side, the hardness is below 300 HV10.

Introduction

The aerospace and automotive industries require components with graded mechanical, thermal, and tribological properties known as functionally graded components. These components provide multi-functional properties suitable for engineering applications. Thermal process control is one common production method for manufacturing tailored parts. In the tool tempering method, a combined die simultaneously has different temperatures on each side. As a result, after forming the blank in the combined die, the microstructure and the mechanical properties of the component at different sections are dissimilar [1].

In the indirect press hardening process, boron alloy steel blanks, mostly 22MnB5, are heated to the austenitization temperature (about 900 °C) and then transferred to the die, where they are cooled using a technique called die quenching, in which the forming and quenching processes occur simultaneously. The high blank temperature reduces the flow stress (lower forming forces) and increases the formability during the forming. The main advantages of this process are the possibility of producing parts with low weight (thin sheets), high strength (approx. 1500 MPa), and low spring back. From a tooling perspective, the key parameter in the press-hardening process is using the enhanced cooling system to achieve a cooling rate of at least 27 K/s [1]. The conventional method for manufacturing press-hardened dies with complex cooling channels includes machining, hardening, and, in most cases, coating. The most common technique is to design press hardening or hot stamping dies by integrating cooling channels drilled in multiple segments of the die body, which are then joined together to form a single unit. However, proper sealing is the main challenge. A further well-established technique is shell cooling, where the intended component is molded to its final shape on a shell die, with cooling fluid passing through the shell and core dies. An additional approach involves casting the die around cooling profiles. The high manufacturing time and cost are the main drawbacks of these methods [2].

Additive manufacturing recently provided the possibility of manufacturing complex shapes that conventional methods cannot produce. The most common additive manufacturing method is powder bed fusion (PBF) to realize the complex conformal cooling channels in the dies or parts. In the PBF, the focused energy source (laser beam or electron beam) melts the powder layer by layer to build the final geometry. Müller et al. [3] have produced a tool insert with numerically optimized cooling channels to develop a new cooling system for hot forming. The die is produced by combining the conventional method and PBF. Gebauer et al. [4] focused on tool optimization for press hardening, where the die has a conformal cooling system. The press hardening experiments were conducted with an additively manufactured (PBF) tool. Yet, the main drawback of the PBF is long manufacturing time.

A solution for rapid tooling is the utilization of sheet lamination. Bryden et al. [5] showed the utilization of complex conformal cooling channels in metal laminated tools for the aerospace industry, where the tools should show a functionality test at 900 °C. The main issues of conventional laminated tooling technology are the poor bonding of laminae, challenges in removing the stair step effect, and hardening of the tool surface. Dardaei Joghann et al. [6] performed an investigation on a combination of the sheet lamination method with the direct energy deposition (DED) process, which is patented by Hölker and Tekkaya [7]. In this process route, the tool's core is manufactured out of laminated sheets, and the laser metal deposition (LMD) process is utilized to reduce the stair-step effect (Fig. 1). This concept is successfully used to manufacture the deep drawing dies. In this method, the hardening step is no longer required, and it allows the placement of the sensors or other functional elements, such as cooling or heating elements, inside the tool during manufacturing.

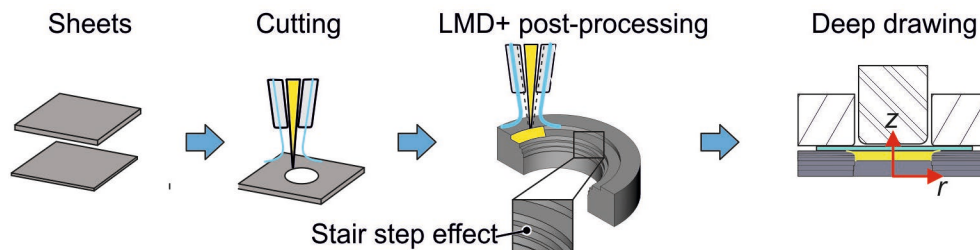


Figure 1: Process route of the hybrid additive laminated tooling [6]

The present work aims to prove the manufacturing tool tempering concept by hybrid additive laminated tooling as introduced in Fig. 1. The main motivation is to manufacture the hybrid die in a short time. For this, a hot stamping insert with the near-surface cooling channels on one side and a warm forming insert with two heating cartridges on the other are manufactured to realize the functionally graded components. The following are the manufacturing and measurement steps, as well as the preliminary results of the formed components.

Experimental work

In all experiments, a 22MnB5 steel sheets with a thickness of 1.5 mm is used as a blank for forming and determining the heat transfer coefficient. The as-received 22MnB5 blank had a hardness of 134 HV10. The ferritic HC420LA (1.0556) sheets are used with thicknesses of 0.5 and 1.0 mm, and the hot-rolled and high-strength steel S355MC (1.0976) with a thickness of 2.0 mm is used as tool laminae. The stair step area is filled with Ferro55 powder (tool steel) with a grain size range of 45 to 80 μm . The chemical composition of the powder is mentioned in Table 1. The laser metal deposition and post-processing are carried out with the Lasertec 65 3D hybrid machine from the company DMG MORI with the laser head COAX14. The laser diameter of 1.6 mm with a focus distance of 7 mm is used.

Table 1: Ferro55 powder chemical composition in weight percentage %

Powder	C	Cr	Mo	Si	Mn	Fe
Ferro55	0.35	7	2.2	0.3	1.1	rest

Determination of the cooling rate and heat transfer coefficient

To determine the effect of the number of deposited layers on the cooling rate and heat transfer coefficient, dies are manufactured with cooling channels and different layers of the depositions with Ferro55 powder (tool steel). Two dies (upper and bottom) are manufactured from horizontally laminated 2 mm thick sheets (S355MC) laser cut by the Trumpf Lasercell 1005 machine available at IUL. The laminated tool is assembled on a 10 mm base sheet (S355MC). Three cooling channels made of copper pipes are used. Since the higher heat transfer can be achieved by a rectangular cooling profile (due to higher contact area), a circular tube with a 12 mm diameter was formed with biaxial compression equipment (self-made at IUL) to $10 \times 10 \text{ mm}^2$ square cross-section profile (**Fig. 2a**). After assembly, the surface of the dies are deposited in three times. The first time, only one layer is deposited. Afterward, the upper and bottom dies are assembled on the Zwick250 universal testing machine from the company Zwick Roell, and the heat transfer coefficient and the cooling rate are determined. Then, the setup is disassembled and placed on the Lasertec 65 machine for the next layer's deposition. This procedure is repeated till the maximum deposition layer of three with a laser power of 800W, feed rate of 1000 mm/min, and powder mass flow of 4 g/min. The deposition area was $72.5 \times 47.5 \text{ mm}^2$. To avoid the thin sheet deformation during the deposition, in-situ cooling is applied to reduce the sheet's thermal deformation. During the experiments, the water is circulated in the cooling channels by cooling aggregate from the company Walter Heller GmbH (**Fig. 2b**). A 4 mm thick cover sheet is also used to reduce the thermal deformation of the thin sheets during the deposition (**Fig. 2c**).

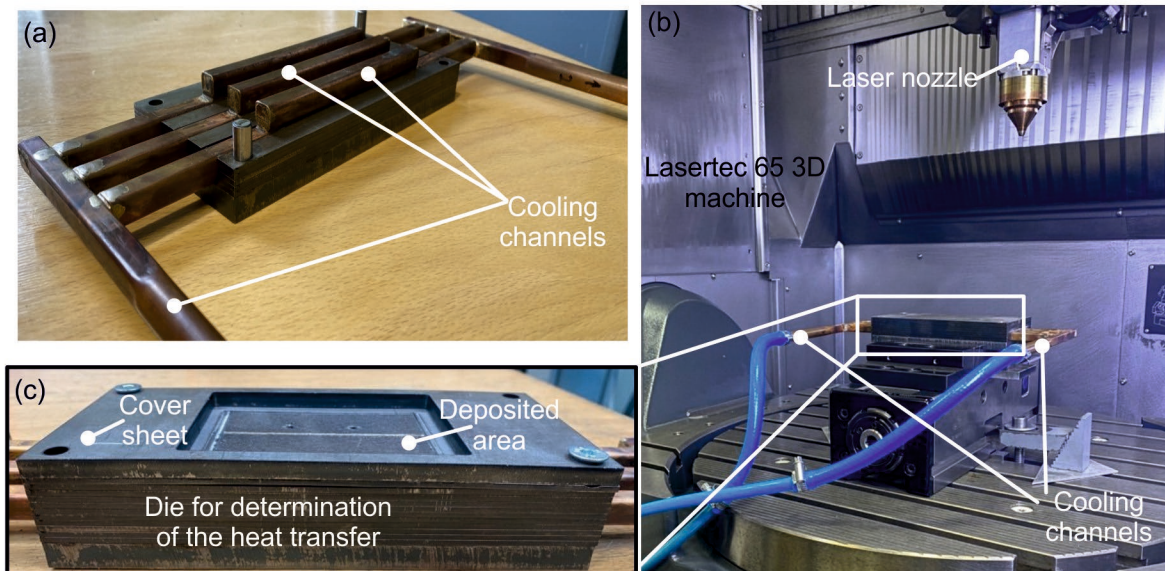


Figure 2: (a) Placing the cooling channels, (b) deposition of the Ferro55 layers on the dies for determination of the coefficient of heat transfer and the cooling rate, (c) using of a cover sheet during the deposition

A self-made setup at IUL is used to determine the cooling rate and the heat transfer coefficient (**Fig. 3**). The whole setup is assembled on the Zwick250, and the 22MnB5 blanks were heated for 5 minutes to austenitization temperature (900 °C) in a Nabertherm N161 furnace. The blanks were then transferred manually to the setup and placed on the bottom die. The transfer and the placement time were under five seconds. The temperature loss by the transport was around 175°C. Then, the

bottom die is closed with a speed of 10 mm/s, and a contact pressure of 10 MPa for 15 seconds is applied. During the experiments, the thermographic camera VarioCam HD head 680 S from the company Infratec GmbH measured the blanks' and dies' temperatures. The emissivity value is experimentally determined and set at 0.85. Type-K thermocouples with a 2 mm diameter also measured the temperature near the surface (0.5 mm distance). The geometrical accuracy measurements of the formed parts were measured by a 3D-Profilometer, VR-5200, from the company Keyence.

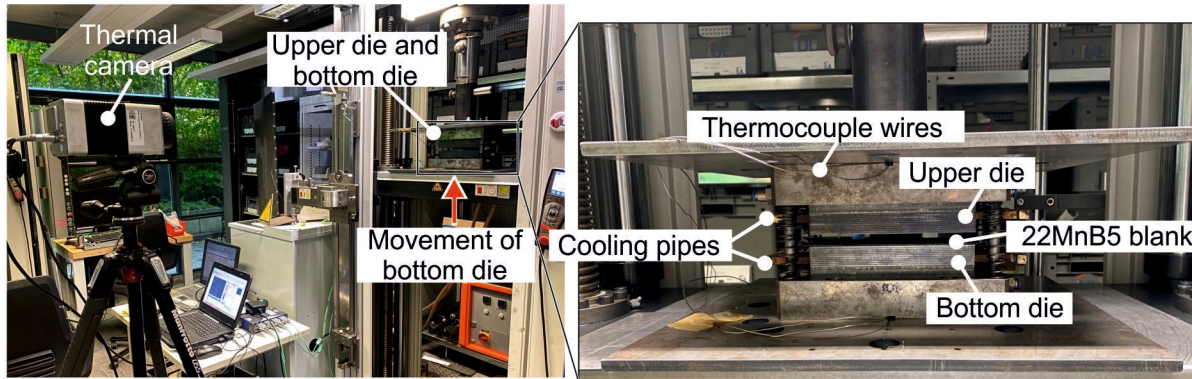
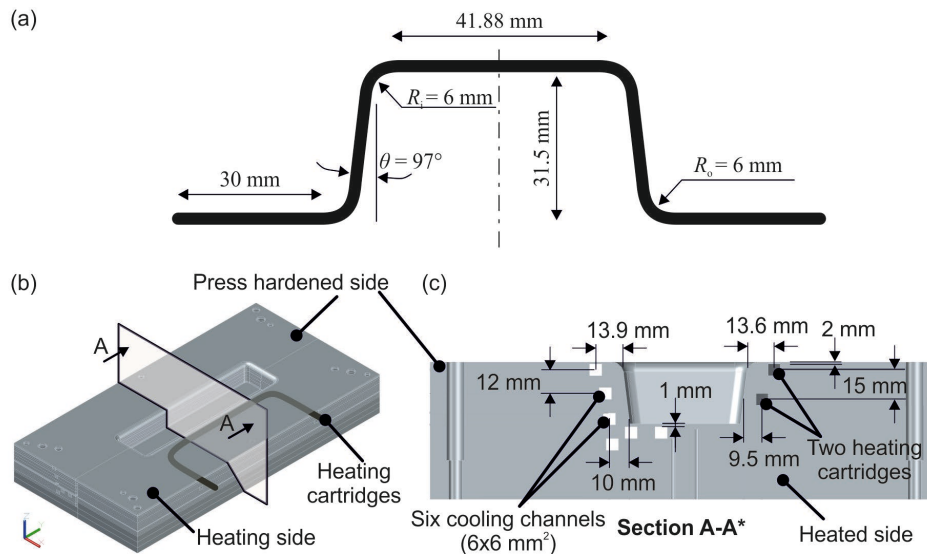


Figure 3: Test setup for determination of the heat transfer coefficient

Manufacturing the hybrid tool

The combined tool (hot stamping and warm forming) is manufactured for the demonstrator component (Fig. 4a) with a radius of 6 mm, as illustrated schematically in Fig. 4b. The position of the six cooling channels with a $6 \times 6 \text{ mm}^2$ square cross-section and the two heating cartridges are shown in Fig. 4c.



*Hatching due to sheet lamination is ignored to better visualize the section.

Figure 4: (a) Nominal geometry for demonstrator component, (b) perspective view of the hybrid tool, (c) cross-section of the hybrid tool

During the placement of cooling channels, the most possible position close to the tool surface is selected. The cooling channels are up to 73% closer to the forming zone than a similar conventionally manufactured die. The laminae are positioned in the proper location with positioning pins. On the heating side, two heating cartridges out of stainless steel with a $6 \times 6 \text{ mm}^2$ square cross-section, a length of 400 mm, and a maximum power of 650W at 230V are placed (Fig. 4c). The cartridges are formable with a minimum bending radius of 23 mm from the company

Heizelemente Industrie Maxi watt. The stair-step areas for both sides are laser metal deposited. As mentioned in [6], a two-step strategy is used for deposition. An offset of 1 mm is applied to ensure enough space to fill the deposited material during the LMD. The process parameters during deposition and laser polishing are in **Table 2**. The die has a corner outer radius $R_o = 6$ mm, so an optimized sheet arrangement based on the economic criterion [8] is used. Using the economic criterion reduces the 520 possible sheet combinations (0.5, 1, and 2 mm sheets) for R_o of 6 mm to 24. The order of the sheets is 1, 1, 0.5, 1, 0.5, and 2 mm (from bottom to top of the tool surface in the radius area). This combination is preferred because it is preferable to have a thicker sheet at the top, as the top sheet is subjected to the highest thermal load during LMD and post-processing (laser polishing). The remaining sections (i.e., after the die corner radius) are discretized to match the cooling channels' preconceived design and the heating cartridges' design. After the deposition of both sides, laser polishing is used to improve the surface roughness with the process parameters in **Table 2**.

Table 2: Process parameters for laser metal deposition and laser polishing

Process	Step	Power P (W)	Feed rate f (mm/min)	Powder mass flow \dot{m} (g/min)
Laser metal deposition	Bonding	1400	1000	7
	Filling	1200	1000	4
Laser polishing	Post-processing	800	400	-

Both sides are assembled on two 10 mm thick base plates (in sum 20 mm thickness). In the separation area of the assembled combined die (except for face sheets), isolator plates were used on both sides to protect the heat exchange with a press-hardened segment (**Fig. 5**).

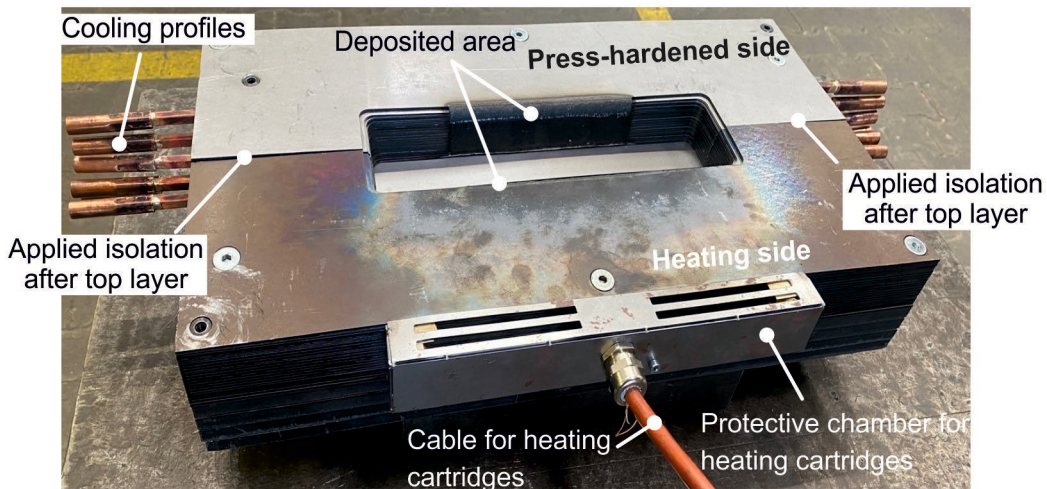


Figure 5: Manufactured hybrid die for the production of the functionally graded components

Forming process

The forming experiments were performed in HYDRAP HPSZK 100-1000/650 hydraulic drawing press with a maximum force of 1000 kN from SCHULER-HYDRAP GmbH & Co. KG. The 22MnB5 blanks with 184×95 mm² dimensions were formed. The blanks were formed at a speed of 30 mm/s with two different blank holder forces, 50 kN and 75 kN. The blanks were heated in a chamber furnace at 900°C for five minutes to ensure complete austenitization (i.e., change in crystal structure from ferrite to austenite) and manually positioned on the die with a temperature drop of 120°C. A contact thermometer is used to monitor the blank temperature before and after forming. A thermal imaging camera is used to observe the temperature in different die sections. Ionized water is pumped through the cooled section of the die. A second pump from Hyfra Industriekühlanlagen GmbH was also used to cool the punch. Due to technical issues, cooling only

one side of the punch was impossible. The blanks were formed and held between the die, punch, and blank holder for 15 seconds. After opening the die, the sheets' temperature is measured at various points. The influence of the three preheating temperature values (150, 250, and 350°C) of the heating side of the combined die on the accuracy of the final part geometry, hardness, and microstructure was investigated.

Results and discussions

Determination of the cooling rate and the heat transfer coefficient

The heat transfer coefficient (α) is calculated based on the Newton's law of cooling as:

$$\alpha = -\ln\left(\frac{T_0 - T_u}{T(t) - T_u}\right) \cdot \frac{c_p \cdot t}{A}, \quad (1)$$

where T_0 is the initial temperature of the blank, and $T(t)$ is the temperature of the blank as a function of time. T_u represents the die temperature on the surface. The time duration of the experiment is represented with t , and A is the contact area. The blank's heat capacity (c_p) is considered 650 J/kgK [9]. The determined heat transfer coefficient (α) and corresponding cooling rate (T') are presented in **Fig. 6**. A steep decrease in α is observed after deposition of the first layer. Increasing the number of layers shows a slow, steady decrease of 10 K/s for the cooling rate. It can be concluded that the deposited Ferro55 has a lower heat transfer coefficient compared to base sheets (S355MC). The cooling rates are still higher than the critical rates of 27 K/s for press hardening.

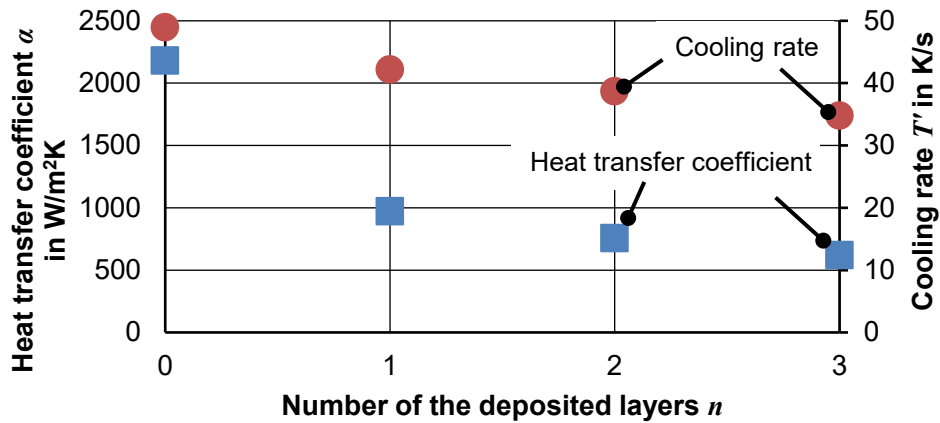


Figure 6: Heat transfer coefficient and cooling rate for die without ($n = 0$) and with several deposition layers

Manufacturing of functionally graded components

Before assembling the two sides of the die on the base plate, the temperature distribution of the heating side is captured by the thermographic camera at different preheating temperatures ($T_0 = 150^\circ C, 250^\circ C,$ and $350^\circ C$), as shown in **Fig. 7**. The temperature distribution is non-uniform in the heating side of the die at the different temperature levels. The top surface shows much lower temperatures than the forming zone. Yet, the temperature distribution is fairly homogeneous across the forming zone (radius area). However, increasing the preheating temperature increases the temperature difference even in the forming zone to ca. $14^\circ C$ (**Fig. 7**).

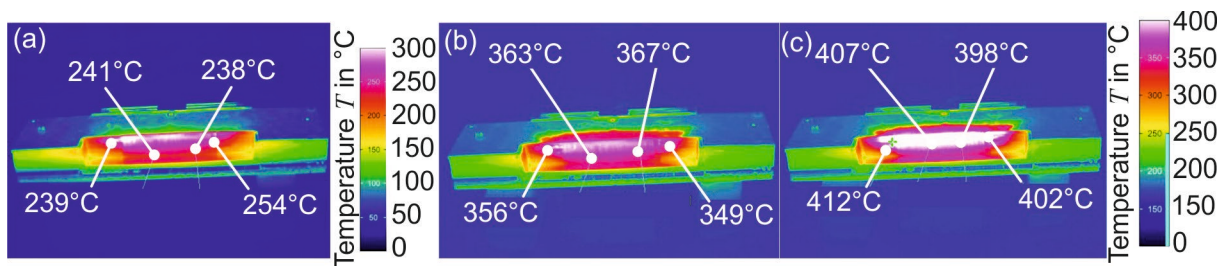


Figure 7: Thermographic camera results for different preheating temperatures (T_0), (a) 150°C, (b) 250°C, (c) 350°C

The initial forming experiments were carried out with the blank holder force of 75 kN with a distance of 1.65 mm between the blank holder and the die. The preheating temperature of the heating side of the die is set to 150°C. It was observed that a fracture had occurred in the formed part during the forming process at the heating side of the die. The blank holder force is reduced to 50 kN to avoid the fracture, and the distance between the die and the blank holder is increased to 1.8 mm. The formed blanks with the new parameters were without any failure. Next, three components were formed for each preheating temperature (T_0). An overview of the tool and specimen temperatures after forming processes is presented in **Table 3**. The small increase in the temperature of the specimen (ca. 9%) on the press-hardened side is due to an increase in the preheating temperature of the heated side. It also led to an increase in the blank holder temperature.

Table 3: Temperature of the tool and blank after forming process

T_0	Die temperature (°C)	Specimen temperature after forming (°C)		Blank holder temperature (°C)
	Press-hardened side	Heating side	Press-hardened side	
150°C	23 ± 1	166 ± 2.5	74 ± 10	41 ± 1
250°C	30 ± 1	181 ± 2.5	79 ± 10	54 ± 0.5
350°C	39 ± 1	197 ± 2.2	81 ± 10	58 ± 1

The geometrical accuracy measurements show that the heating side has a significant effect on the deviation of inclination angle ($\Delta\theta = (\theta - \theta_T) / \theta$, where θ is the nominal angle and θ_T is the angle after the experiment, see **Fig. 4a**), where the press-hardened side shows lower deviation compared to heating side (**Fig. 8a**). The inner radii show significantly lower geometric inaccuracy than the outer radii regardless of the die temperature (errors less than 3%). The reason for higher accuracy is that the inner radius of the specimen is formed by the punch, which is manufactured by the milling process. The outer radius deviation ($\Delta R_o = (R_o - R_T) / R_o$, where R_o is the nominal outer radius, and R_T is the radius after the experiment, shows inaccuracy by a maximum of 8%. Increasing the preheating temperature also leads to an increase in the outer radius deviation (**Fig. 8b**). The hardness (H) value at the different points in the formed part shows a consistent hardness at ca. 480 HV10 (an increase of ca. 260%) except at the specimen wall at all preheating temperatures (**Fig. 9**). At point 3, at all preheating temperatures, the hardness decreases to around 400 HV10, 60% less than in other areas (except point 8). At point 8, the blank is in full contact with the portion of the heated side with the highest temperature during the forming (**Fig. 7**). This results in lower hardness (ca. 280 HV10). However, because of the inhomogeneous temperature distribution on the heating side of the die, the hardness in other areas is the same as quenching.

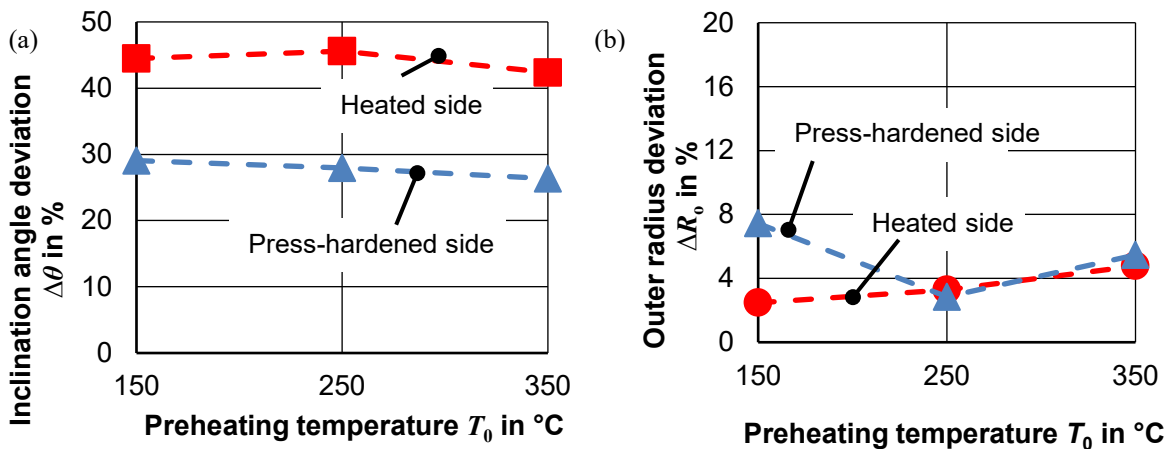


Figure 8: Effect of preheating on (a) inclination angle deviation, (b) outer radius deviation

The other possible reason is due to lower strain hardening due to the variations in strain levels, part-die thermal contact, and consequent cooling rate in the walls of the formed parts as Grydin et al. [10], Taylor and McCulloch [11], and Naderi et al. [12] mentioned. Another reason for the high hardness in the heating area is the usage of the punch with the cooling channel. Since it was not possible to circulate the cooling fluid only in one side of the punch, the phase transformation also happened in this area.

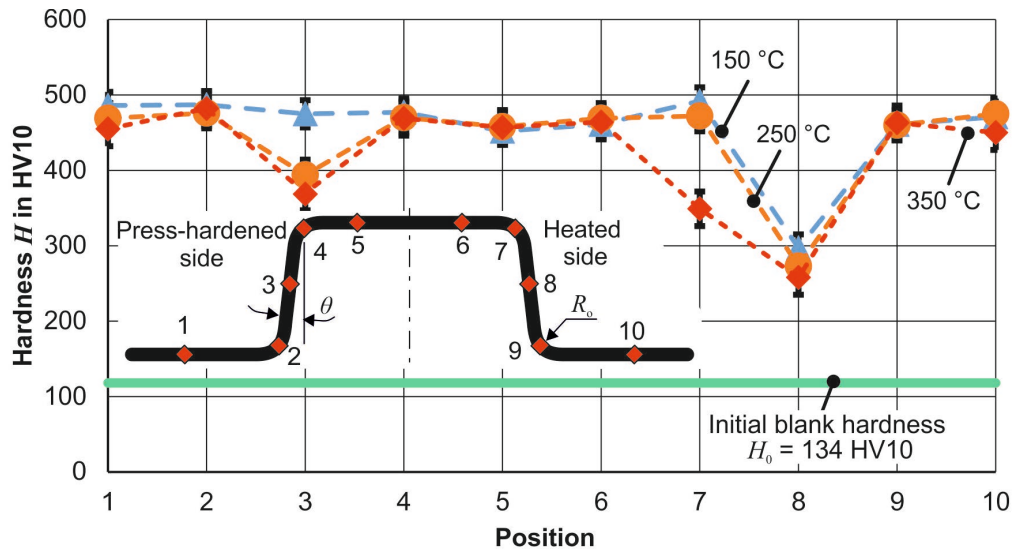


Figure 9: Hardness distribution at different preheating temperatures

The microstructure distribution of the as-received 22MnB5 sheet is the ferritic-pearlitic structure. It consists of interlocked cementite lamellae, which are randomly distributed and oriented in a ferrite matrix (Fig. 10a). At all preheating temperatures, the phase transformation to martensite in the press-hardened section can be observed (Fig. 10b, c, d). However, except for the wall area on the heating side, other areas also have unwanted phase transformation to martensite structure, which confirms the hardness measurements results. Another reason for this unwanted phase transformation is the low preheating temperature, as seen at preheating temperature $T_0 = 150^{\circ}\text{C}$ (Fig. 10b), where the transformation happens even in the wall. The martensite structure in the base and transition zone also explains the high hardness values on the heated side in Fig. 9.

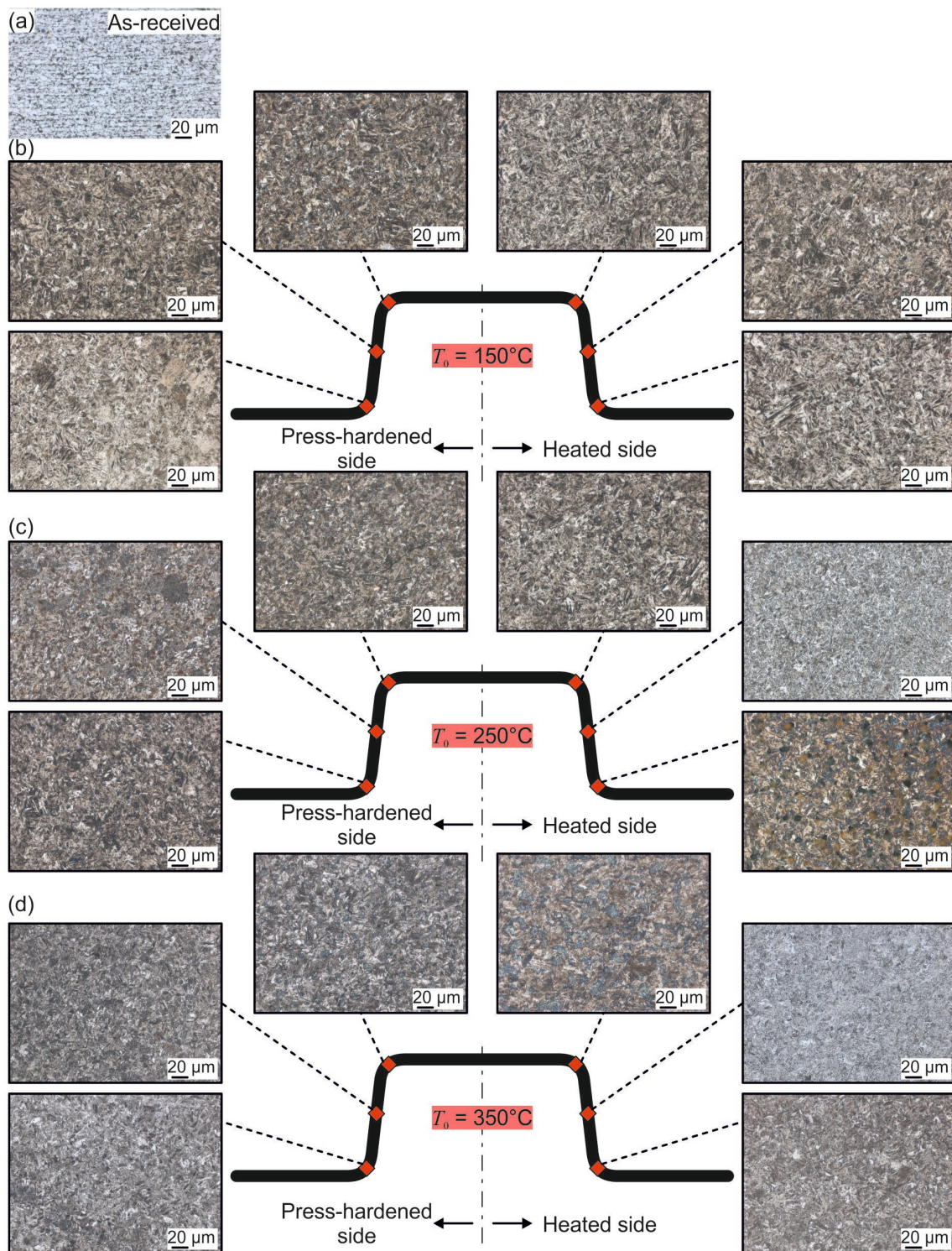


Figure 10: Microstructure of (a) as-received blank, and the formed parts at (b) $T_0 = 150^\circ\text{C}$, (c) $T_0 = 250^\circ\text{C}$, (d) $T_0 = 350^\circ\text{C}$

Summary

The cooling rate and heat transfer coefficient for deposited Ferro55 layers were determined, and it was shown that the cooling rate is sufficiently quick for the press hardening process. The tool for functionally graded components is produced quickly and costlessly without the hardening process by hybrid additive laminated tools, where one side of the tool is equipped with cooling channels and the other with heating cartridges. The application of hybrid additive manufacturing offers the

possibility of positioning the cooling channels nearer to the tool surface while reducing costs compared to conventionally manufactured tools. Although this preliminary study has proven the concept for the production of hybrid tools for functionally graded components, further studies are required to optimize the position and size of the conformal cooling channels and heating cartridges to improve the cooling rate and, at the same time, heating rate.

Acknowledgments

The authors would like to kindly acknowledge the support of the German Research Foundation (DFG) for funding the project “Reducing the stair step effect for dies manufactured by layer-laminated manufacturing by additive and formative post-processing” with funding number 426515407. Mr. Sven Lukies is acknowledged for his technical support with the metallography.

References

- [1] H. Karbasian, A.E. Tekkaya, A review on hot stamping. *J. of Materials Processing Technology*. 210 (2010) 2103-2118. <https://doi.org/10.1016/j.jmatprotec.2010.07.019>
- [2] E. Billur, *Hot Stamping of Ultra High-Strength Steels*, first ed., Springer Cham, 2019. <https://doi.org/10.1007/978-3-319-98870-2>
- [3] B. Müller, M. Gebauer, R. Malek, N. Gerth, Metal Additive Manufacturing for tooling applications Beam Melting technology increases the efficiency of dies and molds. In *Proceedings of the Metal Additive Manufacturing Conference MAMC*, Vienna, Austria, 20–21 November 2014.
- [4] P. Stoll, A. Spierings, M. Gebauer, B. Müller, S. Polster, T. Feld, M. Klinger, A. Zurbrügg, High performance sheet metal forming tooling by additive manufacturing. *Proceedings of the 6th International Conference on Additive Technologies* (2016) 354-361.
- [5] B.G. Bryden, D.I. Wimpenny, I.R. Pashby, Manufacturing production tooling using metal laminations. *Rapid Prototyping Journal* 7 (2001) 52-59.
- [6] H. Dardaei Joghhan, M. Hahn, J. T. Sehart, A. E. Tekkaya, Hybrid additive manufacturing of metal laminated forming tools, *CIRP Annals*, 71(2022), 225-228. <https://doi.org/10.1016/j.cirp.2022.03.018>
- [7] R. Hölker, A. E. Tekkaya, Verfahren zur Reduzierung des Treppenstufenef-fekts bei aus Blechlamellen geschichteten Werkzeugen/Bauteilen mittels additiver und umformtechnischer Nachbearbeitung. German patent DE102018004294 (A1), priority date: 17.05.2018.
- [8] H. Dardaei Joghhan, M. Hahn, O. Agboola, A.E. Tekkaya, Resources and manufacturing technology evaluation of hybrid additive metal laminated tooling for forming. *Materials Research Proceedings*, (2023) 21-30. <https://doi.org/10.21741/9781644902479-3>
- [9] J. Lechler, M. Merklein, M. Geiger, Determination of thermal and mechanical material properties of ultra-high strength steels for hot stamping. *Steel research international*. 79 (2008) 98-104. <https://doi.org/10.2374/SRI07SP131-79-2008-98-104>
- [10] O. Grydin, A. Andreiev, M.J. Holzweißig, C.J. Rüsing, K. Duschik, Y. Frolov, Short austenitization treatment with subsequent press hardening: correlation between process parameters, microstructure and mechanical properties. *Mater Sci Eng A*. 749 (2019), 176-195. <https://doi.org/10.1016/j.msea.2019.02.025>
- [11] T. Taylor, J. McCulloch, Effect of part/die boundary conditions on microstructural evolution during hot stamping 2000 MPa class boron steel. *Steel Res Int*. 89 (2018). <https://doi.org/10.1002/srin.201700495>
- [12] M. Naderi, M. Ketabchi, M. Abbasi, W. Bleck. Analysis of microstructure and mechanical properties of different hot stamped B-bearing steels. *Steel Res Int*. 81 (2010), 216-223. <https://doi.org/10.1016/j.proeng.2011.04.078>